Miscibility and Hydrogen-Bonding Behavior in Organic/Inorganic Polymer Hybrids Containing Octaphenol Polyhedral Oligomeric Silsesquioxane

Ying-Chieh Yen,[†] Shiao-Wei Kuo,[‡] Chih-Feng Huang,[†] Jem-Kun Chen,[§] and Feng-Chih Chang*,[†]

Institute of Applied Chemistry, National Chiao-Tung University Hsin-Chu, Taiwan, Department of Materials and Optoelectronic Engineering, Center for Nanoscience, and Nanotechnology, National Sun Yat-Sen University, Kaohsiung, Taiwan, and Department of Polymer Engineering, National Taiwan University of Science and Technology, Taipei, Taiwan

Received: April 8, 2008; Revised Manuscript Received: May 28, 2008

In this study, we investigated the miscibility behavior and mechanism of interaction of poly(methyl mechacrylate) (PMMA), poly(vinyl pyrrolidone) PVP, and PMMA-*co*-PVP blends with octa(phenol)octasilsequioxane (OP-POSS). For the PMMA/OP-POSS binary blend, the value of the association constant ($K_A = 29$) was smaller than that in the poly(vinyl phenol) (PVPh)/PMMA ($K_A = 37.4$) and ethyl phenol (EPh)/PMMA ($K_A = 101$) blend systems, implying that the phenol groups of the OP-POSS units in the PMMA/OP-POSS blends interacted to a lesser degree with the C═O groups of PMMA than they did in the other two systems. In addition, the ionic conductivity of a $LiClO_4$/PMMA-*co*-PVP polymer electrolyte was increased after blending with OP-POSS.

1. Introduction

Composite materials comprising organic polymers and inorganic materials have attracted great interest in recent years for both their fundamental scientific behavior and industrial applications. Polyhedral oligomeric silsesquoixanes (POSSs), which have the general formula $(RSiO_{1.5})_n$, are prototypical organic/inorganic systems composed of inorganic cores with external organic substituents. Through appropriate designing of the functionality of these organic substituents, it is possible to create both mono- and octafunctional macromonomers for desired applications. These functionalized POSS derivatives can be blended[1−3] or attached covalently to linear thermoplastics[4−11] or thermosetting networks[5,6,12−17] to form high-performance hybrid materials.[18−23] The physical properties of POSS/polymer hybrid materials are strongly influenced by the miscibility of the host polymer and the POSS derivative. Hydrogen bonds are often exploited as a favorable interaction to improve the miscibility of blend systems.[24−26] In a previous study,[27] we observed a dramatic increase in the glass transition temperature when strong hydrogen bonds existed between the POSS moieties and polymer containing proton acceptors.

In this study, the POSS was functionalized as a strong proton donor [i.e., octa(phenol)octasilsesquioxane (OP-POSS)] to improve its miscibility with polymers containing proton acceptors. In previous studies,[27,28] the thermal properties of poly(methyl methacrylate) (PMMA) and poly(vinylpyrrolidone) (PVP) polymers were enhanced through copolymerization with POSS derivatives. Because covalent copolymerization can be a complicated and time-consuming process, polymer blending is usually considered to be a simpler and more convenient means of preparing POSS/polymer hybrid materials. Our aim in this present study was to compare the miscibility and hydrogen-bonding behavior of the PMMA/OP-POSS, PVP/OP-POSS, and PMMA-*co*-PVP/OP-POSS blends. Furthermore, POSS-based electrolytes for rechargeable lithium batteries have been reported:[29] the incorporation of POSS derivatives improved the potential applicability of these systems as solid state electrolytes. Thus, the ionic conductivity of the $LiClO_4$/OP-POSS/PMMA-*co*-PVP ternary blends was also investigated. We employed differential scanning calorimetry (DSC), Fourier transform infrared (FTIR) spectroscopy, and ac impedance measurement as a battery of techniques to investigate the hydrogen-bonding, miscibility, and ionic conductivity behavior of these systems.

2. Experimental Section

Materials. Ethyl ether, benzene, *N,N*-dimethylformamide (DMF), tetrahydrofuran (THF), azobisisobutyronitrile (AIBN), *N*-vinyl-2-pyrrolidone (VP), platinum divinyltetramethyldisiloxane complex [Pt(dvs)], 4-acetoxystyrene (AS), lithium perchlorate ($LiClO_4$), and methyl methacrylate (MMA) were purchased from Aldrich Chemical Co. $Q_8M_8^H$ was obtained from Hybrid Plastics Co. AIBN was purified through recrystallization from ethanol. Benzene and DMF were fractionally distilled from calcium hydride. The MMA and VP monomers were purified through vacuum distillation from calcium hydride. Ethyl ether, THF, $Q_8M_8^H$, Pt(dvs), and AS were used as received.

Synthesis of Octa(phenol)octasilsequioxane-POSS (OP-POSS) Oligomer. The $Q_8M_8^H$ oligomer (1.96 mmol) was placed in a dry 50-mL round-bottom flask equipped with a stirrer bar. Toluene (30 mL), AS (16.66 mmol), and Pt(dvs) (one drop) were added sequentially over 10 min. The reaction mixture was then heated to 80 °C under a nitrogen atmosphere for 4 h. After cooling to room temperature, the solution was filtered and then evaporated, and finally the residue was dried under vacuum until reaching a constant weight. The product, octa(acetoxystyryl)-octasilsequioxane (AS-POSS, Scheme 1, yield was calculated to be 80%), was obtained as a colorless, viscous liquid.[30] AS-POSS was dissolved in THF under a nitrogen atmosphere and then NaOH (10%) was added dropwise. The mixture was stirred for 48 h at room temperature. After the reaction, ethyl ether and deionized water (1:1) were added, and then aqueous

* To whom all correspondence should be addressed. Tel: 886-3-5131512. Fax: 886-3-5131512. E-mail: changfc@mail.nctu.edu.tw.
[†] National Chiao-Tung University Hsin-Chu.
[‡] National Sun Yat-Sen University.
[§] National Taiwan University of Science and Technology.

10.1021/jp8030495 CCC: $40.75
Published on Web 08/13/2008

SCHEME 1: Synthesis and Chemical Structure of OP-POSS

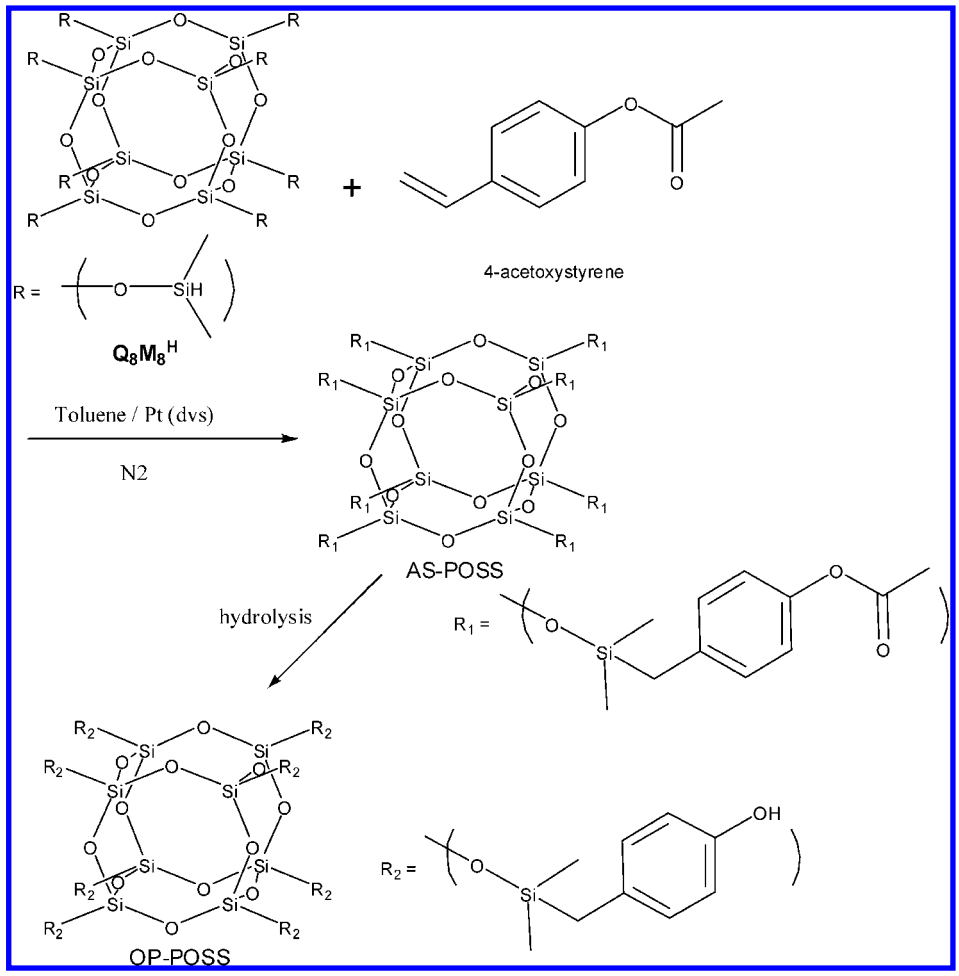

hydrochloric acid (10%) was added dropwise to the mixture with stirring until the pH reached 8. Residual ethyl ether and water were evaporated under vacuum to provide octa(phenol)octasilsequioxane (OP-POSS, yield was calculated to be 82%). The final product, OP-POSS (Scheme 1), which is a lightly brown and viscous liquid, was filtered and dried in a vacuum oven for 96 h at 80 °C.[30]

Syntheses of PMMA-*co*-PVP Random Copolymers. The PMMA-*co*-PVP random copolymers were prepared through the free radical polymerization using AIBN as the initiator (Scheme 2) The reactions were performed in benzene at 80 °C under a nitrogen atmosphere in a dry 100-mL round-bottom flask equipped with a stirrer bar. To determine the reactivity ratio, samples of the copolymers were removed from the reaction mixture during the early stages of the copolymerization, when the degrees of conversion remained relatively low (between 4 and 9%).[31] After 24 h, the mixtures were cooled to room temperature and the product copolymers were purified through precipitation into ethyl ether. The filtered product copolymers were dried until they reached a constant weight. The molecular weights and molecular weight distributions of the PMMA-*co*-PVP copolymers were characterized through GPC at 50 °C using DMF as the eluent and polystyrene standards for calibration. The compositions of the copolymers were characterized using ^{1}H NMR spectroscopy and elementary analysis (EA).

The ^{1}H NMR spectrum of the copolymer was recorded from a $CDCl_3$ solution at 25 °C using a Varian UNITY INOVA-400 NMR spectrometer. EA was performed in an oxidative atmosphere at 1021 °C using a Heraeus CHN-O Rapid Elementary

SCHEME 2: Synthesis of PMMA-*co*-PVP Random Copolymer

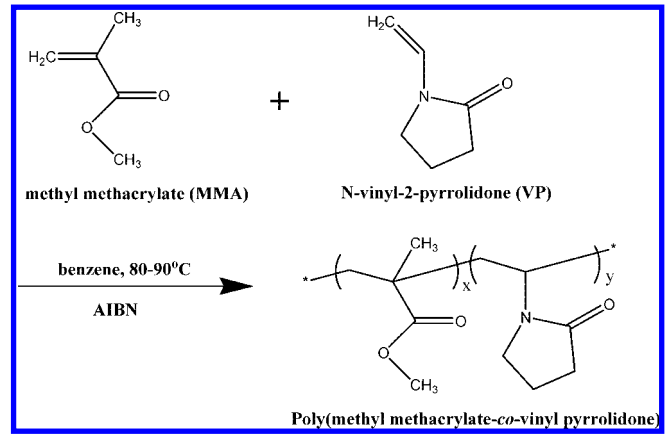

Analyzer. The MMA and VP units in the PMMA-*co*-PVP copolymers correspond to repeating units of $C_5H_8O_2$ and C_6H_9NO, respectively; thus, the MMA content (mol %) was determined using eq 1, based on the contents of C and N atoms.[32]

$$\text{MMA (mol \%)} = 1 - \frac{30N}{7C - 6N} \times 100 \qquad (1)$$

where N and C refer to the contents of N and C atoms, respectively, in the copolymer.

Blend Preparations. Several binary PMMA/OP-POSS, PVP/OP-POSS, and PMMA-*co*-PVP/OP-POSS blends were prepared.

TABLE 1: PMMA-*co*-PVP Copolymer Compositions and Molecular Weights[a]

	monomer feed (mol %)		polymer composition (mol %) EA[c]		polymer composition (mol %) NMR[d]				
copolymer abbreviation[b]	VP	MMA	VP	MMA	VP	MMA	M_n[e]	M_w/M_n[e]	T_g[f] (°C)
PMMA	0	100	0	100	0	100	25 700	1.76	111
MMA81	18.4	81.6	19.4	80.6	18.7	81.3	22 100	2.00	123
MMA61	37.5	62.5	38.5	61.5	40.7	59.3	20 300	2.52	134
MMA53	47.4	52.6	46.8	53.2	52.9	47.1	17 000	2.29	139
PVP	100	0	100	0	100	0	18 200	2.33	181

[a] Polymerization conditions: initiator = AIBN, solvent = benzene, temperature = 80 °C. [b] Labeling based on VP content in the PMMA-*co*-PVP copolymers obtained from EA. [c] Calculated through EA using eq 1. [d] Obtained from the ^{1}H NMR spectra. [e] Determined by GPC using polystyrene standards and DMF as the eluent. [f] Characterized from DSC thermograms.

Desired amounts of PMMA, PVP, PMMA-*co*-PVP, and OP-POSS were dissolved in DMF and stirred continuously for 24 h at 60 °C. The solutions were cast into Teflon dishes and maintained at 80 °C for 24 h to remove most of the solvent and then the blends were dried under vacuum maintained at 120 °C for 96 h.

Characterizations. Thermal analyses were performed using a DuPont TA2010 DSC instrument calibrated with indium standards. The analyses were conducted under a nitrogen atmosphere at a scan rate of 20 °C/min over a temperature range from −60 to 200 °C. The glass transition temperature (T_g) was obtained as the inflection point of the heat capacity jump. FTIR spectra of KBr disks were recorded over the range 4000−400 cm^{-1} using a Nicolet Avatar 320 FT-IR spectrometer, and 32 scans were collected, at room temperature and a resolution of 1 cm^{-1}. Each DMF solution was cast onto a KBr disk and then most of the solvent was evaporated at 80 °C for 24 h; a vacuum (0.2 Torr) was applied and the blend was then heated at 120 °C for an additional 96 h to completely remove the solvent. The frequency-dependent impedance properties (from 10 MHz to 10 Hz) of the polymer complexes were measured using an Autolab instrument designed by Eco Chemie. The samples were pressed into disks and loaded into a sealed conductivity cell between stainless-steel blocking electrodes; the films had thicknesses varying from 0.50 to 0.15 mm for these conductivity measurements. The impedance response was measured at 30 °C and the conductivity was calculated from the bulk resistance according to the eq 2[33,34]

$$\sigma = \frac{L}{AR_b} \tag{2}$$

where σ is the conductivity, L is the thickness of the electrolyte film, A is the section area of the stainless-steel electrode, and R_b is the bulk resistance.

3. Results and Discussion

PMMA-*co*-PVP Copolymer Characterization. A series of copolymers was prepared using various VP and MMA monomer concentrations. Table 1 lists the MMA contents (mol %) of the copolymers, determined through ^{1}H NMR spectroscopy and EA. Because the compositions of the copolymers determined through ^{1}H NMR spectroscopy were affected by the interaction between water and PMMA-*co*-PVP, their VP contents (mol %) are slightly overestimated. EA provided better accuracy, although the H atom contents determined this way are inaccurate because compositions of the copolymers were affected by the presence of water. Accordingly, we applied only the EA-determined N and C contents to calculate the VP content using eq 1. In the following discussion, the sample codes for these copolymers are based on the MMA contents obtained through EA.

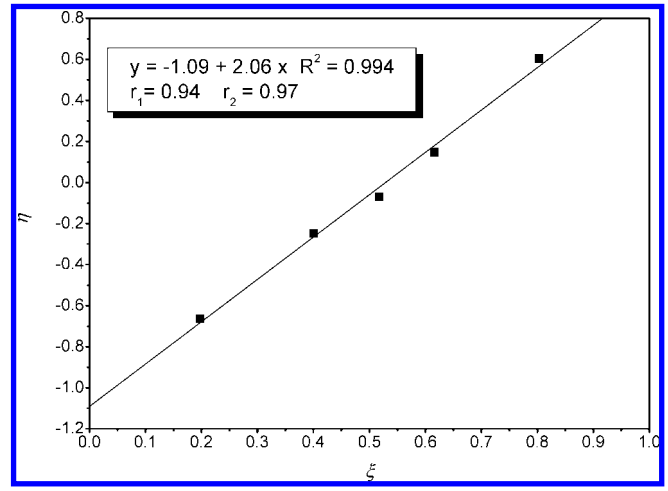

Figure 1. Kelen−Tudos plot for the PMMA-*co*-PVP copolymers.

We calculated reactivity ratios (r_1 for MMA and r_2 for VP) using the methodology of Kelen and Tudos.[35−37] Table 1 summarizes the monomer feed ratios and the resultant compositions of the copolymers. To minimize errors that resulted from changes in the feed ratios, the polymerization was terminated at monomer conversions of less than 10%. The values of r_1 and r_2 are the ratios of the homopropagation and cross-propagation rate constants for each monomer (i.e., k_{11}/k_{12} and k_{22}/k_{21}, respectively). Figure 1 displays the Kelen−Tudos plot for the PMMA-*co*-PVP copolymers. The values of r_1 and r_2 were 0.94 and 0.97, respectively. In a previous study,[38] we defined a copolymerization to be "ideal" when the product r_1r_2 was unity. When r_1 and r_2 both equal 1, the two monomers possess equal reactivity toward both propagating species; the behavior of the resulting copolymer is referred to as random or Bernoullian behavior. Thus, the copolymers synthesized through free radical polymerization in this study were essentially random. (i.e., close to an ideal copolymer: $r_1r_2 = 0.91$).

Analyses of OP-POSS/Homopolymer Binary Blends. Figure 2 presents DSC thermograms of the PMMA/OP-POSS and PVP/OP-POSS blends. The star-shaped OP-POSS was similar to a linear oligomer of poly(vinyl phenol); i.e., it has a degree of polymerization equal to 8. The glass transition temperature of OP-POSS (25 °C) was lower than that of a typical high molecular weight (M_n = 10 000 g/mol) PVPh (150 °C) because of molecular weights and structural differences. Single values of T_g existed in both blends, implying that all of these binary and ternary blends are miscible. Several equations have been suggested to predict the variation of the glass transition temperature of a random copolymer or miscible blend as a function of its composition. In this study, we employed the Kwei equation to predict the variation of the glass transition temperature:

$$T_g = \frac{W_1 T_{g1} + kW_2 T_{g2}}{W_1 + kW_2} + qW_1 W_2 \quad (3)$$

where W_1 and W_2 are the weight fractions of the compositions, T_{g1} and T_{g2} represent the glass transition temperature of the corresponding blend components, and k and q are fitting constants. Furthermore, the value of q, a parameter corresponding to the strength of hydrogen bonds in the blend, correlated to the balance between the breaking of the self-association and the formation of the interassociating hydrogen bonds. Figure 3 displays the dependence of T_g on the compositions of the PVP/OP-POSS and PMMA/OP-POSS blends. We obtained the values of k and q based on nonlinear least-squares best fits. In the PVP/OP-POSS blends, q had a value of +100, revealing the presence of a strong intermolecular interaction between PVP and OP-POSS. On the other hand, a negative value of q (−40) was obtained for the PMMA/OP-POSS blends, indicating that the intermolecular hydrogen bonding was weaker than the intramolecular hydrogen bonding.

Figure 4 displays partial IR spectra (2700−3700 cm^{-1}) of the PMMA/OP-POSS and PVP/OP-POSS blends. The pure OP-POSS exhibits two bands in the OH stretching region in the IR spectrum, one corresponding to the hydrogen-bonded OH groups (a broad band centered at 3350 cm^{-1}) and the other to "free" OH groups (a shoulder centered at 3525 cm^{-1}). When the PMMA (PVP) was mixed with OP-POSS and the C═O oxygen atoms of PMMA (PVP) interacted with the OH groups of OP-POSS, the broad band shifted to higher (lower) frequency at 3450 (3190) cm^{-1}. This behavior reflected the competition between the hydroxyl−hydroxyl and hydroxyl−carbonyl inter-

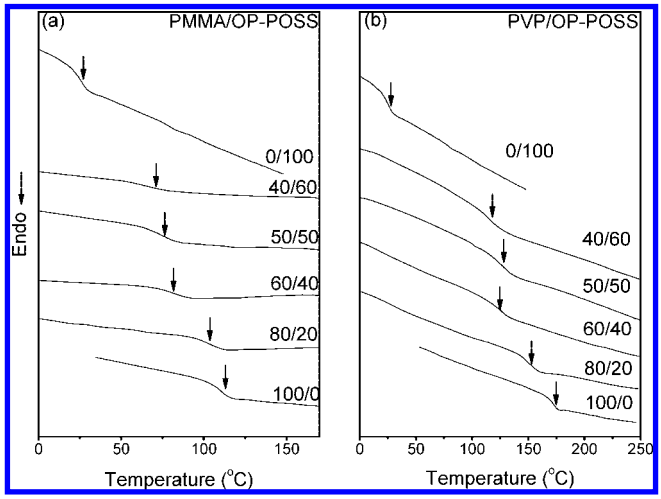

Figure 2. DSC scans for (a) PMMA/OP-POSS and (b) PVP/OP-POSS blends of various compositions.

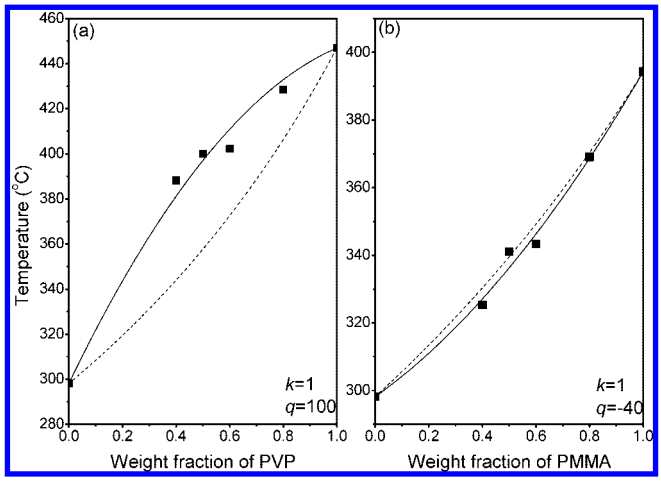

Figure 3. Plots of T_g versus (a) the PVP content of PVP/OP-POSS blends and (b) the PMMA content of PMMA/OP-POSS blends.

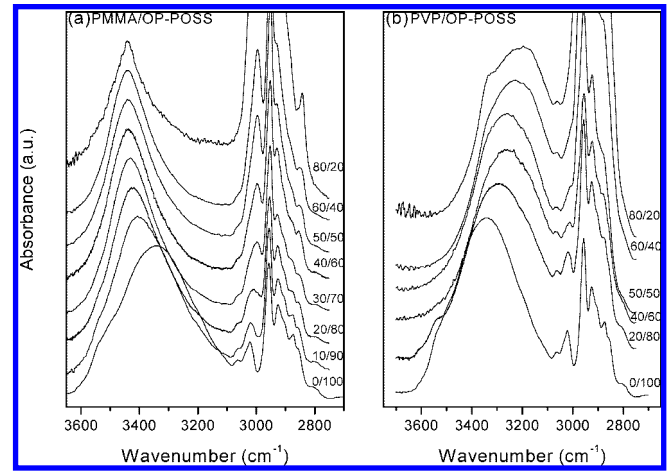

Figure 4. Partial IR spectra (OH stretching region) of OP-POSS and P MMA/OP-POSS and PVP/OP-POSS blend systems.

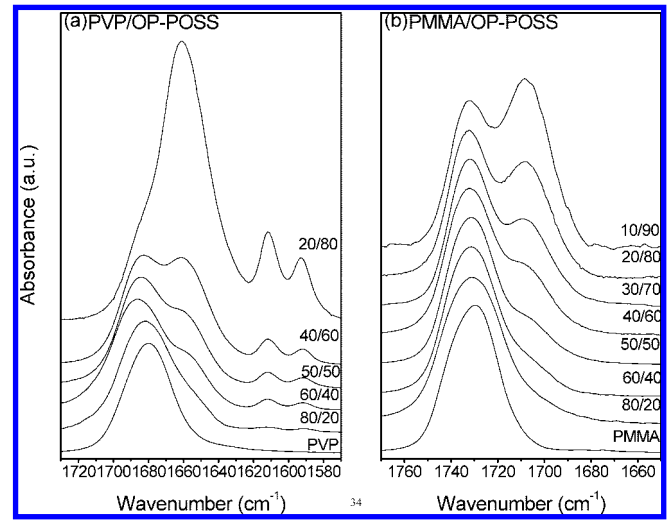

Figure 5. Partial IR spectra (C═O stretching region) of (a) PVP/OP-POSS blends at 120 °C and (b) PMMA/OP-POSS blends at 25 °C.

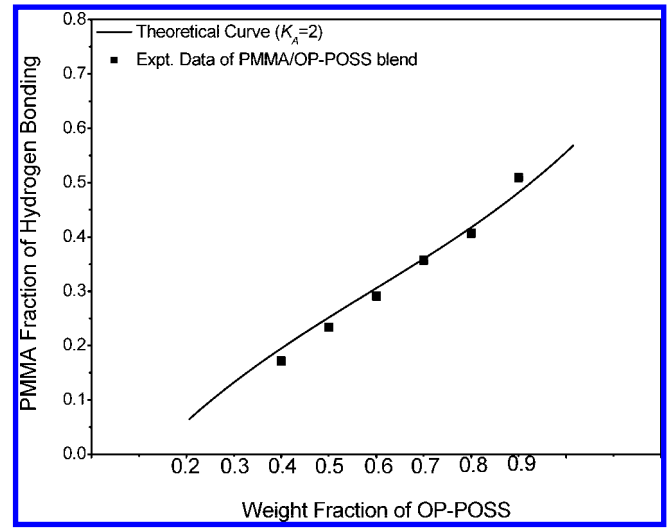

Figure 6. Fraction of the hydrogen-bonded C═O groups plotted with respect to the blend composition: (■) FTIR spectroscopy data and (—) theoretical values for PMMA/OP-POSS blends (K_A = 2) at 25 °C.

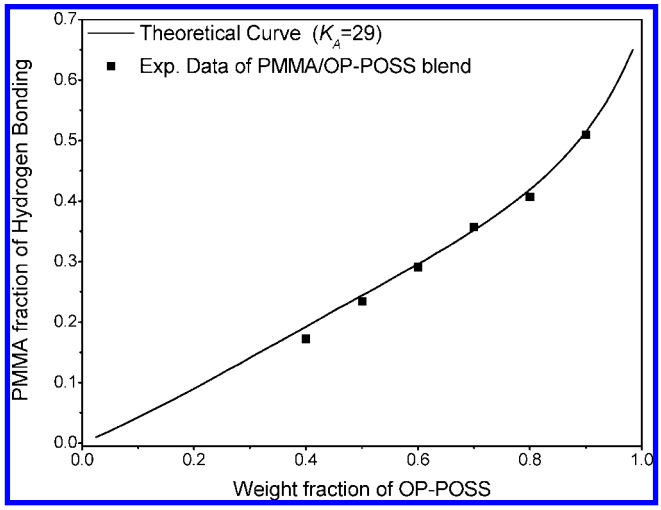

Figure 7. Fraction of the hydrogen-bonded C═O groups plotted with respect to the blend composition: (■) FTIR spectroscopy data and (—) theoretical values for PMMA/OP-POSS blends (K_A = 29) at 25 °C.

TABLE 2: Curve Fitting of the C═O Stretching Bands in the FTIR Spectra of PVP/OP-POSS and PMMA/OP-POSS Blends at Room Temperature

	free C═O			hydrogen-bonded C═O			
	ν, cm^{-1}	$W_{1/2}$, cm^{-1}	A_f %	ν, cm^{-1}	$W_{1/2}$, cm^{-1}	A_b %	f_b
			PVP/POSS				
pure PVP	1680	28	100				
80/20	1681	31	91.5	1652	18	8.5	6.7
60/40	1685	31	82.8	1653	20	17.2	13.8
50/50	1685	28	67.5	1656	22	32.5	27.0
40/60	1687	23	40.9	1659	28	59.1	52.6
20/80	1690	15	5.9	1660	30	94.1	92.5
			PMMA/POSS				
PMMA	1730	20	100				
80/20	1731	21	85.8	1707	25	14.2	10.0
60/40	1732	22	76.3	1707	24	23.7	17.2
50/50	1732	20	68.6	1708	24	31.4	23.4
40/60	1732	19	61.9	1708	23	38.1	29.1
30/70	1732	18	54.6	1708	23	45.4	35.7
20/80	1732	17	49.3	1708	23	50.7	40.7
10/90	1732	18	39.2	1708	23	60.8	50.9

TABLE 3: Self-Association and Interassociation Equilibrium Constants and Thermodynamic Parameters for PMMA/OP-POSS Blends at 25 °C[a]

			equilibrium constant		
	V	M_w	K_2[b]	K_B[b]	K_A[c]
OP-POSS	1705.2	1978	21.0	66.8	
PMMA	84.9	100			29.0

[a] V, molar volume (mL/mol); M_w, molecular weight (g/mol); K_2, dimer self-association equilibrium constant; K_B, multimer self-association equilibrium constant; K_A, interassociation equilibrium constant. [b] Reference 40. [c] Calculated using the PCAM.

actions. Additionally, the hydroxyl−carbonyl interactions predominated over the hydroxyl−hydroxyl interactions in the PMMA (PVP)-rich blends; thus, we assigned the band at 3450 (3190) cm^{-1} to be the OH groups interacting with the C═O units. Moskala et al. used the frequency difference ($\Delta\nu$) between the hydrogen-bonded and free OH absorptions to estimate the average strength of the intermolecular interaction.[39] Accordingly, we used the free OH stretching at 3525 cm^{-1} as a reference, the hydroxyl−carbonyl interassociation was weaker than the hydroxyl−hydroxyl self-association interaction in the PMMA/

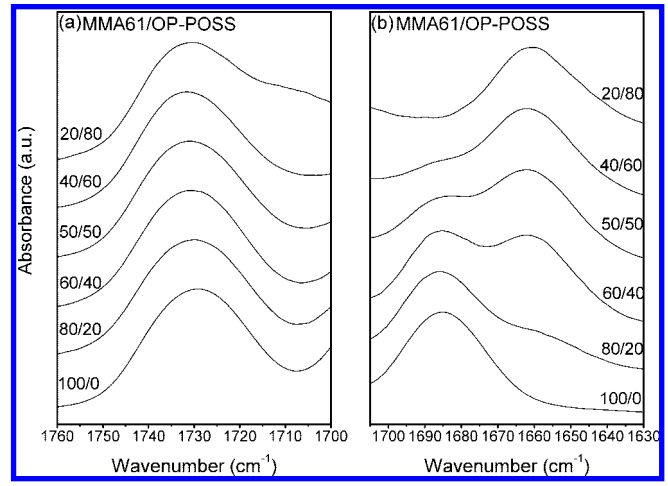

Figure 8. Partial IR spectra (1800−625 cm^{-1}) of the MMA61/OP-POSS blend containing various OP-POSS contents, recorded at 120 °C.

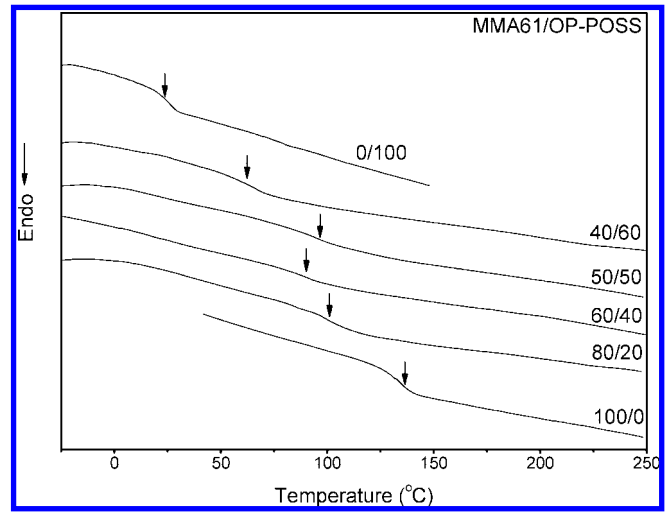

Figure 9. DSC scans for MMA61/OP-POSS blends of various compositions.

OP-POSS blends, but stronger in the PVP/OP-POSS blends. This finding is consistent with the negative and positive values of q for the PMMA/OP-POSS and PVP/OP-POSS blends, based on the Kwei equation.

Figure 5 displays the C═O stretching regions in the IR spectra of PVP/OP-POSS and PMMA/OP-POSS blends. In Figure 5a, pure PVP exhibits a broad band centered at 1680 cm^{-1}, corresponding to the "free" C═O groups. Painter et al.[40] reported that the pyrrolidone group strongly self-associates through transitional dipole coupling. Therefore, the signal for "free" C═O groups at 1680 cm^{-1} is not that of "truly free" C═O groups, which would be centered at 1708 cm^{-1}. The signal for C═O stretching was split into two bands at 1680 and 1650 cm^{-1}, corresponding to "free" and hydrogen-bonded C═O groups, respectively; these signals fitted the Gaussian function well. As the concentration of OP-POSS increased, the probability of PVP/OP-POSS interactions increased, resulting in an increased intensity of the hydrogen-bonded C═O band at the expense of the "free" C═O band. We calculated the fraction of the hydrogen-bonded C═O groups (f_b) using eq 4[41]

$$f_b^{C=O} = \frac{A_b/1.3}{A_b/1.3 + A_f} \quad (4)$$

where A_b and A_f denote the peak areas corresponding to the hydrogen-bonded and "free" C═O groups, respectively. In this

TABLE 4: Curve Fitting of the C=O Stretching Bands in the FTIR Spectra of MMA61/OP-POSS (120°C) Blends

	free C=O			hydrogen-bonded C=O				free C=O			H-bonded C=O			
	ν, cm^{-1}	$W_{1/2}$, cm^{-1}	A_f, %	ν, cm^{-1}	$W_{1/2}$, cm^{-1}	A_b, %	f_b	ν, cm^{-1}	$W_{1/2}$, cm^{-1}	A_f, %	ν, cm^{-1}	$W_{1/2}$, cm^{-1}	A_b, %	f_b
MMA61	1683	25	100					1730	26	100				
80/20	1686	26	75.1	1658	23	24.9	20.2	1730	28	100				
60/40	1686	25	49.0	1660	24	51.0	44.5	1730	27	93.0	1710	20	7.0	4.7
50/50	1687	26	42.9	1659	24	57.1	50.5	1730	26	90.6	1710	20	9.4	6.5
40/60	1687	26	28.3	1660	25	71.7	66.1	1730	26	85.4	1710	20	14.6	10.2
20/80	1687	25	10.9	1660	25	89.1	86.3	1730	26	75.7	1710	20	24.3	17.6

case, we employed a ratio for the two absorptivities (a_2/a_1) of 1.3 based on a previous calculation.[40] Table 2 summarizes the results of curve fitting for the PVP/OP-POSS blends. As expected, the fraction of hydrogen-bonded C=O groups increased upon increasing the OP-POSS content.

Figure 5b reveals that the PMMA blend system has a sharp (compared with that of the pure PVP) IR band at 1730 cm^{-1} and a shoulder at 1710 cm^{-1}, representing the free and the hydrogen-bonded C=O groups, that also fitted the Gaussian function well. We applied the method described above to analyze the PMMA/OP-POSS blends, but in this case, we used a value of a_2/a_1 of 1.5.[42] Table 2 lists the results of curve fitting of the PMMA/OP-POSS system. Again, the fractions of hydrogen-bonded C=O groups increased upon the increase of the OP-POSS content.

In previous studies,[27,28] we confirmed that certain interactions occur between the POSS moieties and OH group. In this study, the situation was more complicated than those in previous studies because the OH groups were attached to the POSS cage. To further understand the interaction phenomena, we employed the Painter−Coleman association model (PCAM) to analyze these systems[41]

$$B_1 + B_1 \overset{K_2}{\longleftrightarrow} B_2 \tag{5}$$

$$B_h + B_1 \overset{K_B}{\longleftrightarrow} B_{h+1}\ (h \geq 2) \tag{6}$$

$$B_h + C_1 \overset{K_c}{\longleftrightarrow} B_hC \tag{7}$$

$$B_h + A_1 \overset{K_A}{\longleftrightarrow} B_hA \tag{8}$$

where A, B, and C are descriptors representing the siloxane groups, the phenol groups of the POSS cages, and PMMA, respectively; K_A, K_B, and K_C are their respective association equilibrium constants; K_2 is the equilibrium constant of forming dimers between phenol groups. These equilibrium constants can be expressed in terms of volume fractions

$$\Phi_B = \Phi_{B1}\Gamma_2\left[1 + \frac{K_A\Phi_{A1}}{r_A} + \frac{K_C\Phi_{C1}}{r_C}\right] \tag{9}$$

$$\Phi_A = \Phi_{A1}[1 + K_A\Phi_{B1}\Gamma_1] \tag{10}$$

$$\Phi_C = \Phi_{C1}[1 + K_C\Phi_{B1}\Gamma_1] \tag{11}$$

$$\Gamma_1 = \left(1 - \frac{K_2}{K_B}\right) + \frac{K_2}{K_B}\left(\frac{1}{1 - K_B\Phi_{B1}}\right) \tag{12}$$

$$\Gamma_2 = \left(1 - \frac{K_2}{K_B}\right) + \frac{K_2}{K_B}\left(\frac{1}{(1 - K_B\Phi_{B1})^2}\right) \tag{13}$$

where Φ_A, Φ_B, and Φ_C are the volume fractions of the repeat units in the blend; Φ_{A1}, Φ_{B1}, and Φ_{C1} are the volume fractions of the isolated units in the blend; and r_A (V_A/V_B) and r_C (V_C/V_B) are the ratios of the segmental molar volumes.[28] Furthermore, we adopted the self-association equilibrium constants of PVPh[45] ($K_2 = 21$ and $K_B = 66.8$) for phenol groups in this study to describe the formation of dimers and multimers, respectively. The interassociation equilibrium constant (K_C) of the PVPh/PMMA blend has been reported previously to be 37.4.[44] Using the value of K_C together with the phenol group self-association equilibrium constants (K_2 and K_B), we obtained a theoretical curve for the fraction of hydrogen-bonded C=O groups at 25 °C as a function of the weight fraction of OP-POSS content (Figure 6) When the value of K_A was equal to 2, the experimental data agreed fairly well with the predictions of the PCAM. A slight deviation was observed at weight fractions less than 0.4, because the most accurate range for determining the fraction of hydrogen-bonded C=O groups was from 0.4 to 0.7, where the bands for both the free and hydrogen-bonded C=O bands were well-separated and had significant absorbances.[45] The ratio of the interassociation equilibrium constant (K_A) corresponding to the interaction between OH and siloxane groups of POSS cages to the interassociation equilibrium constant (K_C) was 0.05, implying that interassociation between the phenol and siloxane groups of the POSS cages was insignificant and, thus, could be ignored. The structure of the OP-POSS and the hydroxyl−hydroxyl interaction formed through the phenol groups are the reasons for this behavior because both the arms of OP-POSS, which were steric barriers, and the presence of hydroxyl−hydroxyl interaction blocked the OH groups from interacting with the siloxane groups.

Using the value of the K_B and K_2 above and ignoring interassociation between the phenol and siloxane groups of OP-POSS, we employed the PCAM again to determine the "real" value of K_A for the PMMA/OP-POSS blend. The approximate equations were simplified as follows:[46,47]

$$\Phi_B = \Phi_{B1}\Gamma_2\left[1 + \frac{K_A\Phi_{A1}}{r_A}\right] \tag{14}$$

$$\Phi_A = \Phi_{A1}[1 + K_A\Phi_{B1}\Gamma_1] \tag{15}$$

where

$$\Gamma_1 = \left(1 - \frac{K_2}{K_B}\right) + \frac{K_2}{K_B}\left(\frac{1}{(1 - K_B\Phi_{B1})}\right) \tag{16}$$

$$\Gamma_2 = \left(1 - \frac{K_2}{K_B}\right) + \frac{K_2}{K_B}\left(\frac{1}{(1 - K_B\Phi_{B1})^2}\right) \tag{17}$$

where Φ_A and Φ_B denote the volume fractions of the non-self-associated species A (PMMA) and the self-associating species B (OP-POSS), respectively; Φ_{A1} and Φ_{B1} are the corresponding volume fractions of the isolated PMMA and OP-POSS, respectively; r is the ratio of molar volumes (V_A/V_B). Using the least-

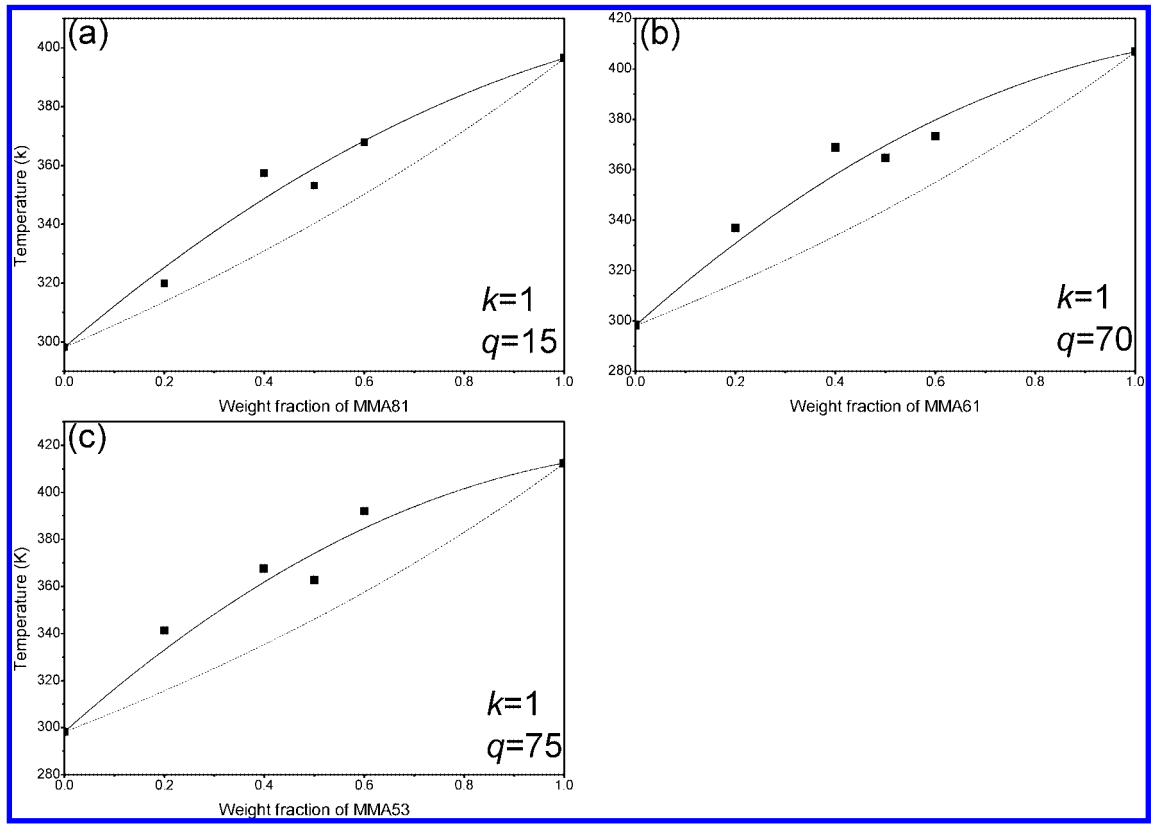

Figure 10. Plots of T_g versus (a) the MMA81 content of MMA81/OP-POSS blends, (b) the MMA61 content of MMA61/OP-POSS blends, and (c) the MMA53 content of MMA53/OP-POSS blends.

squares method, we obtained theoretical curves for the fraction of hydrogen-bonded C═O groups at 25 °C as a function of the weight fraction of the OP-POSS content (Figure 7) When K_A was equal to 29.0, the experimental data agreed fairly well with the predictions of the PCAM. Table 3 lists all the parameters required for the PCAM to estimate the thermodynamic properties of these blends. Furthermore, the interassociation equilibrium constant (K_A = 29.0) of the PMMA/OP-POSS blend system was smaller than that of the self-association equilibrium constant (66.8) of the OP-POSS oligomer; this finding implies that the tendency toward self-association of two OH groups dominates over the hydroxyl−carbonyl interactions in the PMMA/OP-POSS blends. Most importantly, the value of K_A for PMMA/OP-POSS blend system was smaller than those for poly(vinyl phenol) PVPh/PMMA (K_A = 37.4)[44] and ethyl phenol (EPh)/PMMA (K_A = 101)[48] blends, implying that the OH groups in the PMMA/OP-POSS blend system have less of a chance to interact with C═O groups than they do in the other two blends. In a previous study,[44] we found that the value of the interassociation equilibrium constant is affected by the spacing between the hydrogen-bonding functional groups. In this case, the spacing between the OH groups attached to the POSS cage (a star-shaped macromolecule) can be smaller than those of the other two blend systems, making them less accessible for interassociation, resulting in a decrease in the ratio of the interassociation and self-association equilibrium constants.

We could not, however, use this approach to determine the K_A for the PVP/OP-POSS blend because the pyrrolidone groups exhibited strong self-association through transitional dipole coupling and the signal for "free" carbonyl group at 1680 cm^{-1} was not that of "truly free" C═O groups, which would have been centered at 1708 cm^{-1}. Furthermore, for the value of K_A for the PVP/OP-POSS blends to be calculated accurately, it would have to be less than 6000 ± 2000 based

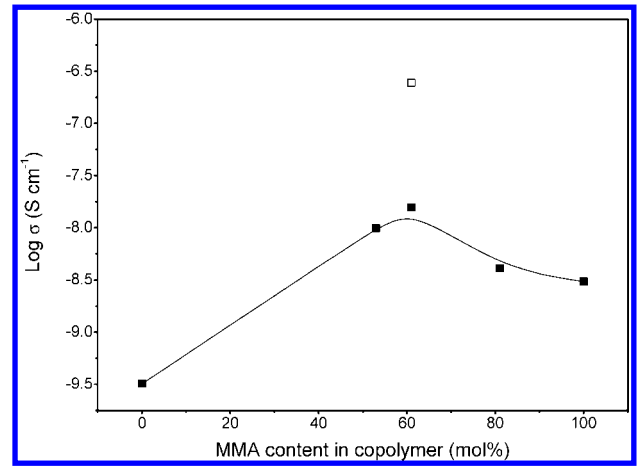

Figure 11. Plots of ionic conductivity with respect to the MMA content in PMMA-*co*-PVP copolymers for (■) $LiClO_4$/polymer binary blends and (□) $LiClO_4$/OP-POSS/MMA61 ternary blends.

on the results above.[40] In previous studies,[49−51] we determined that the value of q for the PMMA/PVPh and PVP/PVPh blend systems were 0 and 140, respectively—much greater than those of −40 and 100 for the PMMA/OP-POSS and PVP/OP-POSS blend systems, respectively—indicating that the intermolecular hydrogen bonding in the PMMA/OP-POSS and PVP/OP-POSS blends was weaker than that in the PMMA/PVPh and PVP/PVPh blends. The values of K_A are in good agreement with these results obtained from curve fitting of the Kwei equation.

Analyses of Binary Blend OP-POSS/Copolymers. Figure 8 displays the C═O regions for the MMA and VP units in the IR spectra of the MMA61/OP-POSS blend. Table 4 summarizes the results of curve fitting. The addition of a small content of

OP-POSS (20%) in the blend resulted in a new band at 1658 cm^{-1} assigned to the "hydrogen-bonded" C═O groups of the PVP. The signal for the "hydrogen-bonded" C═O groups of PMMA appeared when the OP-POSS content was increased to 40 wt %. The OH groups of OP-POSS prefer to interact with PVP rather than with PMMA, as evidenced by the difference between the value of K_A for the PMMA/OP-POSS and PVP/OP-POSS blend systems. When the OP-POSS content was greater than 40%, the OH groups interacted simultaneously with both the PMMA and PVP units.

As indicated in Table 1, the presence of VP units in each copolymer system resulted in an increase in the value of T_g with all of the DSC traces revealing a single glass transition temperature, implying that these copolymers are miscible. Figure 9 presents DSC thermograms of the MMA61/OP-POSS blend system. Essentially all of the blends displayed the same trend; the presence of OP-POSS results in a lowering of the glass transition temperature of the copolymer. We used the Kwei equation to predict the variation of the glass transition temperature of the miscible blend as a function of its composition. Figure 10 illustrates the dependence of T_g on the composition of the MMA81/OP-POSS, MMA61/OP-POSS, and MMA53/OP-POSS miscible blends. Again, based on the nonlinear least-squares best fit, the values of k and q were obtained. For the MMA53/OP-POSS blend system, we obtained the largest value of q (75), implying that the MMA53/OP-POSS blend system featured stronger intermolecular interactions between OP-POSS and itself than did the other two copolymer/OP-POSS blends. As indicated in Figure 10, the addition of a lower content of VP (20 wt %) in the PMMA chain resulted in a change in nature of the interaction. The intermolecular hydrogen bonds in the PMMA/OP-POSS blends were weaker than the intramolecular hydrogen bonds. After copolymerization at a 20 wt % VP content, the intermolecular hydrogen bonding became stronger than the intramolecular hydrogen bonding because the OH groups interacted more preferably with the VP segments. Therefore, the value of q increased gradually upon increasing copolymerized-VP content, reflecting the fact that the intermolecular hydrogen bonding of the copolymer/OP-POSS blend system became stronger accordingly.

Analyses of Ionic Conductivity. In a previous study,[34] we found that a polymer electrolyte composed of $LiClO_4$/MMA61 had a higher ionic conductivity at room temperature than did the $LiClO_4$/PMMA, $LiClO_4$/PVP, $LiClO_4$/MMA81, and $LiClO_4$/MMA53 blend systems at the same $LiClO_4$ content. As mentioned above, the interactions between polymer chains are affected by the presence of OP-POSS. In addition, because the mobility of charge carriers is directly related to the mobility of the polymer matrix, we were interested in comparing the ionic conductivity of ternary and binary blends. Figure 11 displays the plots of the ionic conductivity with respect to the MMA content in copolymers at room temperature for $LiClO_4$/PMMA-*co*-PVP and $LiClO_4$/OP-POSS/PMMA-*co*-PVP blends containing a fixed $LiClO_4$ content of 20 wt %. The polymer electrolyte $LiClO_4$/OP-POSS/MMA61 exhibited a higher ionic conductivity at room temperature than did the binary blend of $LiClO_4$/PMMA-*co*-PVP because the OP-POSS might lead to an increase in the chain mobility of the polymer electrolyte. To clarify the complicated nature of the interactions in the $LiClO_4$/OP-POSS/polymer ternary blend, we are presently performing additional studies that we will discuss in the near future.

4. Conclusions

We have employed DSC and FTIR spectroscopy techniques to investigate in detail the miscibility behavior and mechanisms of interaction for polymer blends of OP-POSS and PMMA-*co*-PVP. For the OP-POSS/PMMA blends, the value of $K_A = 29$ was smaller than those for the PVPh/PMMA ($K_A = 37.4$) and EPh/PMMA ($K_A = 101$) blends, implying that the spacing between phenol groups attached to the POSS nanoparticle was smaller than those of the other two blend systems, resulting in a decrease in the ratio of the interassociation and self-association equilibrium constants. Moreover, intermolecular hydrogen bonding became stronger than intramolecular hydrogen bonding after copolymerization with VP content because the OH groups preferred to interact with the VP segments. Furthermore, the presence of OP-POSS in a $LiClO_4$/OP-POSS/MMA61 ternary blend played an important role in enhancing the ionic conductivity of the polymer electrolyte.

References and Notes

(1) Kuo, S. W.; Lin, H. C.; Huang, W. J.; Huang, C. F.; Chang, F. C. *J. Polym. Sci., Polym. Phys.* **2006**, *44*, 673.
(2) Lee, Y. J.; Huang, J. M.; Kuo, S. W.; Chang, F. C. *Polymer* **2005**, *46*, 10056.
(3) Zhang, H.; Kulkarni, S.; Wunder, S. L. *J. Phys. Chem. B* **2007**, *111*, 3583.
(4) Kopesky, E. T.; Haddad, T. S.; Cohen, R. E.; McKinley, G. H. *Macromolecules* **2004**, *37*, 8992.
(5) Li, G. Z.; Wang, L.; Toghiani, H.; Daulton, T. L.; Koyama, K.; Pittman, C. Y. *Macromolecules* **2001**, *34*, 8686.
(6) Matejka, L.; Strachota, A.; Plestil, J.; Whelan, P.; Steinhart, M.; Slouf, M. *Macromolecules* **2004**, *37*, 9449.
(7) Lin, H. C.; Wang, C. F.; Kuo, S. W.; Tung, P. H.; Huang, C. F.; Lin, C. H.; Chang, F. C. *J. Phys. Chem. B* **2007**, *111*, 3404.
(8) Leu, C. M.; Chang, Y. T.; Wei, K. H. *Chem. Mater.* **2003**, *15*, 2261.
(9) Leu, C. M.; Chang, Y. T.; Wei, K. H. *Chem. Mater.* **2003**, *15*, 3721.
(10) Phillips, S. H.; Haddad, T. S.; Tomcrzak, S. J. *Curr. Opin. Solid State Mater. Sci.* **2004**, *8*, 21.
(11) Li, G. Z.; Wang, L. C.; Ni, H. L. *J. Inorg. Organomet. Polym.* **2001**, *11*, 123.
(12) Chen, W. Y.; Wang, Y. Z.; Kuo, S. W.; Huang, C. F.; Tung, P. H.; Chang, F. C. *Polymer* **2004**, *45*, 6897.
(13) Tamaki, R.; Choi, J.; Laine, R. M. *Chem. Mater.* **2003**, *15*, 793.
(14) Lee, Y. J.; Huang, J. M.; Kuo, S. W.; Lu, J. S.; Chang, F. C. *Polymer* **2005**, *46*, 173.
(15) Ye, Y. S.; Chen, W. Y.; Wang, Y. Z. *J. Polym. Sci., Part A: Polym. Chem.* **2006**, *44*, 5391.
(16) Liu, Y. L.; Chang, G. P.; Hsu, K. Y.; Chang, F. C. *J. Polym. Sci., Part A: Polym. Chem.* **2006**, *44*, 3825.
(17) Do Carmo, D. R.; Paim, L. L.; Dias, N. L. *Appl. Surf. Sci.* **2007**, *253*, 3683.
(18) Voronkov, M. G.; Lavrent'ev, V. I. *Top. Curr. Chem.* **1982**, *102*, 199.
(19) Baney, R. H.; Itoh, M.; Sakakibara, A.; Suzuki, T. *Chem. Rev.* **1995**, *95*, 1409.
(20) Provatas, J. G. *Trends Polym. Sci.* **1997**, *5*, 327.
(21) Loy, D. A.; Shea, K. J. *Chem. Rev.* **1995**, *95*, 1431.
(22) Lichtenhan, J. D. In *Polymeric Materials Encyclopedia*; Salamone, J. C., Ed.; CRC Press: Boca Raton, FL, 1996, p 7768.
(23) Ni, Y.; Zheng, S. *Chem. Mater.* **2004**, *16*, 5141.
(24) Kuo, S. W.; Chang, F. C. *Macromolecules* **2001**, *34*, 4089.
(25) Kuo, S. W.; Lin, C. L.; Chang, F. C. *Polymer* **2002**, 3943.
(26) Eastwood, E.; Viswanathan, S.; O'Brien, C. P.; Kumar, D.; Dadmun, M. D. *Polymer* **2005**, 3957.
(27) Xu, H. Y.; Kuo, S. W.; Chang, F. C. *Macromolecules* **2002**, *35*, 8788.
(28) Huang, C. F.; Kuo, S. W.; Huang, W. J.; Chang, F. C. *Macromolecules* **2006**, *39*, 300.
(29) Maitra, P.; Wunder, S. L. *Electrochem. Solid-State Lett.* **2004**, *7* (4), A88.
(30) Lin, H. C.; Kuo, S. W.; Huang, C. F.; Chang, F. C. *Macromol. Rapid Commun.* **2006**, *27*, 537.
(31) Xu, Y.; Painter, P. C.; Coleman, M. M. *Polymer* **1993**, *34*, 3010.
(32) Luo, L.; Ranger, M.; Lessard, D. G. ; Le Garrec, D.; Gori, S.; Leroux, J. C.; Rimmer, S.; Smith, D. *Macromolecules* **2004**, *37*, 4008.
(33) Watanabe, M.; Ohashi, S.; Sanui, K.; Ogata, N.; Kobayashi, T.; Ohtaki, Z. *Macromolecules* **1985**, *18*, 1945.
(34) Chiu, C. Y.; Yen, Y. J.; Chang, F. C. *Polymer* **2006**, *48*, 1329.

(35) Kennedy, J. P.; Kelen, T.; Tüdös, F. J. *Polym. Sci., Polym. Chem. Ed.* **1975**, *13*, 2277.
(36) Kelen, T.; Tüdös, F. *Macromol. Sci. Chem.* **1975**, *A9*, 1.
(37) Kuo, S. W.; Chang, F. C. *Polymer* **2001**, *42*, 9843.
(38) Odian, G. *Principles of Polymerization*, 4th ed.; John Wiley & Sons: New York, 2004.
(39) Moskala, E. J.; Varnell, D. F.; Coleman, M. M. *Polymer* **1985**, *26*, 228.
(40) Hu, Y.; Motzer, H. R.; Etxeberria, A. M.; Fernandez-Berridi, M. J.; Iruin, J. J.; Painter, P. C.; Coleman, M. M. *Macromol. Chem. Phys.* **2000**, *201*, 705.
(41) Coleman, M. M.; Graf, J. F.; Painter, P. C. *Specific Interactions and the Miscibility of Polymer Blends*; Technomic Publishing: Lancaster, PA, 1991.
(42) Moskala, E. J.; Howe, S. E.; Painter, P. C.; Coleman, M. M. *Macromolecules* **1984**, *17*, 1671.
(43) Kuo, S. W.; Chan, S. C.; Chang, F. C. *Polymer* **2002**, *43*, 3653.
(44) Lin, C. L.; Chen, W. C.; Liao, C. S.; Su, Y. C.; Huang, C. F.; Kuo, S. W.; Chang, F. C. *Macromolecules* **2005**, *38*, 6435.
(45) Coleman, M. M.; Pehlert, G. J.; Painter, P. C. *Macromolecules* **1996**, *29*, 6820.
(46) Lee, Y. J.; Kuo, S. W.; Huang, W. J.; Lee, H. Y.; Chang, F. C. *J. Polym. Sci.* **2004**, *42*, 1127.
(47) Kuo, S. W.; Chang, F. C. *Macromol. Chem. Phys.* **2002**, *203*, 868.
(48) Hu, Y.; Painter, P. C.; Coleman, M. M.; Butera, R. J. *Macromolecules* **1998**, *31* (10), 3394.
(49) Lee, H. F.; Kuo, S. W.; Chang, F. C. *Macromolecules* **2006**, *39*, 5458.
(50) Chen, W. C.; Kuo, S. W.; Jeng, U. S.; Chang, F. *C Macromolecules* **2008**, *41*, 1401.
(51) Kuo, S. W.; Chang, F. C. *Macromolecules* **2001**, *34*, 4089.

JP8030495